COMPDYN 2025
10th ECCOMAS Thematic Conference on
Computational Methods in Structural Dynamics and Earthquake Engineering
M. Papadrakakis, M. Fragiadakis (eds.)
Rhodes Island, Greece, 15-18 June 2025

DJURA GROUND MOTION RECORD SELECTOR: A SOFTWARE SOLUTION FOR EARTHQUAKE ENGINEERING

Davit Shahnazaryan[1,3], Volkan Ozsarac[1,3], and Gerard J. O'Reilly[2,3]

[1] Postdoctoral Researcher, Centre for Training and Research on Reduction of Seismic Risk (ROSE Centre), Scuola Universitaria Superiore IUSS Pavia, Italy
{davit.shahnazaryan, volkan.ozsarac}@iusspavia.it

[2] Associate Professor, Centre for Training and Research on Reduction of Seismic Risk (ROSE Centre), Scuola Universitaria Superiore IUSS Pavia, Italy
gerard.oreilly@iusspavia.it

[3] Djura | Risk - Data - Engineering, Pavia, Italy
{davit.shahnazaryan, volkan.ozsarac, gerard.oreilly}@djura.it

Abstract

Recent advancements in computational power have led to the increased use of nonlinear response history analysis in seismic design and assessment. A crucial step in these analyses is selecting and scaling appropriate ground motion records. However, engineers rarely use state-of-the-art record selection methods due to the lack of accessible, efficient software tools. To address this gap, a new user interface (UI)-based software for ground motion record selection is introduced. In addition to traditional building code-compliant methods, the software incorporates the generalised conditional intensity measure (GCIM) framework, enabling record selection from harmonized databases like PEER NGA-West2, along with corresponding scale factors. This approach facilitates the simultaneous consideration of multiple ground motion intensity measures through cross-correlation matrices. The software also allows for the inclusion of multiple causal earthquakes and ground motion prediction equations (GMPEs), similar to probabilistic seismic hazard analysis (PSHA). A demonstration of the tool's application is provided, utilising a generalized GMPE to streamline the record selection process. The UI is designed for ease of use, offering flexibility in switching between selection methods and managing input and output data. The tool supports the selection of both horizontal and vertical ground motion components. A case study compares the performance of conditional and unconditional selection methods, with results validated through hazard consistency checks.

Keywords: ground-motion selection; conditional selection; unconditional selection; code-based selection; graphical user interface.

1 INTRODUCTION

Careful selection of ground motion records is crucial in seismic design and assessment, as it significantly affects the accuracy and reliability of performance evaluations. This process starts by establishing a reference point, a "target", which can take different forms such as the design response spectrum outlined in building codes, a uniform hazard spectrum (UHS) derived from probabilistic seismic hazard analysis (PSHA) [1], or a weighted combination of response spectra from earthquake scenarios based on a specific spectral acceleration (SA) value ([2], [3]). Once the target is defined, record selection algorithms are employed to identify a set of ground motion records that closely align with it, ensuring that the chosen records meet the required criteria. For the case of conditional spectrum (CS), the selected records must also preserve hazard consistency by aligning with probabilistic hazard curves across different spectral acceleration periods. Over the years, researchers have proposed numerous methods to enhance the selection process, aiming to capture both the central tendency and variability of response spectra to improve the reliability of seismic assessments (e.g., [4], [5]).

Most ground motion record selection methods traditionally rely on elastic spectral accelerations. However, the severity of ground motion is influenced by multiple factors, including velocity, duration, and frequency content, among others, which are not directly captured by spectral acceleration-based IMs. Recognizing the limitations of conventional selection approaches, Bradley ([6], [7]) introduced the Generalized Conditional Intensity Measure (GCIM) framework, which enables the distribution of a ground motion intensity measure (IM) to be determined based on the values of other non-spectral IMs. When first introduced, a characteristic viewed as a limitation of GCIM was its dependence on ground motion models (GMMs) and correlations between the IMs considered, which restricted the number of IMs it could consider, as GMMs were neither widely available nor developed for alternative IMs. However, advancements in GMMs have since turned this initial constraint into a major advantage.

Recent research has focused on how alternative next-generation IMs can vastly improve the efficiency of structural response prediction and address other issues of bias and sufficiency. For example, the notion of using average spectral acceleration (Sa_{avg}) has been studied by several researchers in the past [e.g., [8]–[13]], exhibiting promising results that make it a strong candidate for improved and more refined assessment methodologies [e.g., [14], [15]]. Similarly, a novel IM termed filtered incremental velocity (FIV3) has been proposed [16] and shown to exhibit quite efficient and sufficient response prediction [e.g., [17], [18]]. However, while these IMs are indeed quite efficient, there often tends to be a lack of practicality that allows their full implementation in engineering practice.

Recent developments in hazard and ground motion tools have produced GMMs tailored for both cumulative intensity-based IMs (e.g., significant duration) and amplitude-based IMs (e.g., spectral acceleration), with these models predicting IMs independently ([19]–[22], among others). Further innovation has focused on next-generation IMs, such as FIV3 [23] and Sa_{avg} [24], both of which have demonstrated strong efficiency and sufficiency ([13], [16], [25]). Additionally, Aristeidou et al. [26] proposed a GMM capable of predicting multiple IMs within a single model, significantly expanding the applicability of the GCIM approach. These advancements have reinforced GCIM as a powerful tool for ground motion selection, enabling a more comprehensive and probabilistically consistent approach to seismic hazard assessment.

In additional to GMMs, the availability of correlation models between various IMs or between different spectral ordinates of the same IM was required. The correlations are important to derive conditional distribution of one IM based on others, especially when employing GCIM. To address this requirement, Aristeidou et al. [27] developed correlation models that

incorporate both traditional IMs such as spectral acceleration, peak ground acceleration, peak ground velocity, and significant duration as well as next-generation IMs like *FIV*3 and Sa_{avg}.

With advancements in computational power, alongside improvements in GMMs, correlation models, and ground motion selection methodologies, non-linear response history analysis has gained prominence in seismic design and assessment. Today, it is the preferred method for design verification and seismic performance evaluation among engineers, owing to its accuracy and ability to provide deeper insights into structural behaviour under earthquake loading. However, despite these advancements, practitioners seldom adopt sophisticated record selection techniques due to the absence of user-friendly and efficient software tools, despite the drawbacks of code-based selection being well-known for years [e.g., [28]] and more advanced methods being permitted by codes such as the revised Eurocode 8 [29]. For this purpose, this paper introduces a user interface (UI)-based software tool designed to facilitate ground motion record selection. In addition to the traditional approaches that strictly follow building code requirements selecting horizontal ground motion components, this tool offers expanded functionality by enabling the selection of vertical ground motion components and integrating the GCIM framework for record selection. It allows users to select records from harmonized databases such as PEER NGA-West2 [30] while simultaneously determining appropriate scale factors. By leveraging cross-correlation matrices, the tool enables the consideration of multiple IMs within a single selection process. Additionally, it supports multiple causal earthquake scenarios and various GMMs, aligning with standard PSHA practices. The software's capabilities are demonstrated through an application of a generalized GMM [26], showcasing its efficiency and practicality in record selection.

2 PROBABILISTIC SEISMIC HAZARD ANALYSIS

First, a target response spectrum is needed for ground motion record selection. A widely adopted method for defining the target spectrum involves conducting PSHA. This requires rupture parameters (*rup*) and GMMs (*gmm*), which are used within a logic tree framework. The logic tree itself is employed to account for and quantify epistemic uncertainty in the PSHA inputs. Figure 1(left) provides an example of the logic tree, illustrating how multiple GMMs are applied to model two distinct rupture scenarios in developing a target spectrum. The probabilities (*p*) of *rups* sum to unity, and similarly, the weights of the *gmm*s (*w*) for a given rupture also sum to unity. Throughout this document, it is assumed that rupture parameters and their corresponding GMMs for each relevant IM are predefined and readily available, as obtained through PSHA disaggregation. Figure 1(right) presents a sample disaggregation output, demonstrating how hazard contributions from different seismic sources are accumulated by summing the contributions of magnitude-distance bins to the overall hazard. In this specific example, the dominant contribution comes from an earthquake with a magnitude of 7.38 occurring at a distance of 1 km. This assumption ensures that multiple rupture scenarios and their respective GMMs are appropriately considered in the calculations, in line with standard PSHA practices.

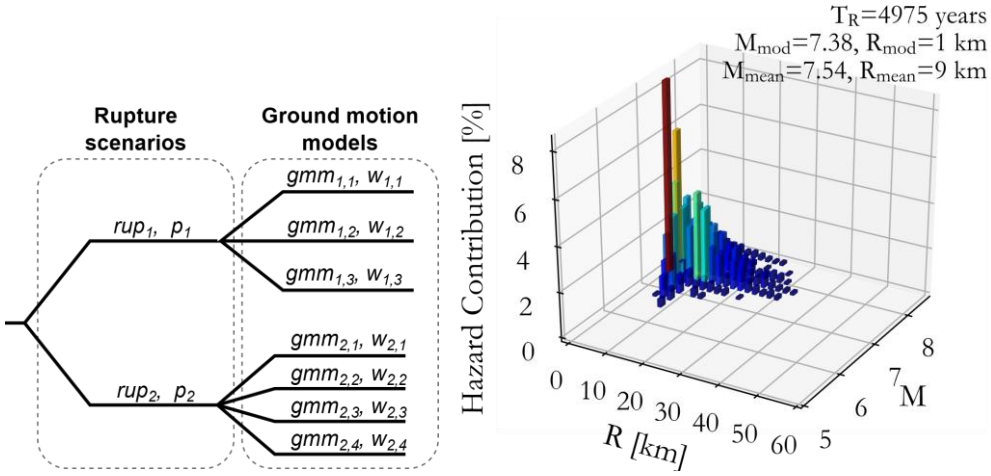

Figure 1. (left) Example logic tree structure for PSHA, and (right) example illustration of disaggregation results from PSHA.

3 TARGET IDENTIFICATION

3.1 Unconditional spectrum

Having defined the logic tree, the unconditional mean and variance for an approximate case with only a single rupture scenario and GMM are computed using Eq. (1) and Eq. (2).

$$\mu_{\ln IM_i} = \mu_{\ln IM_i^g|rup_r} \tag{1}$$

$$\sigma^2_{\ln IM_i} = \sigma^2_{\ln IM_i^g|rup_r} \tag{2}$$

where $\mu_{\ln IM_i^g|rup_r}$ and $\sigma^2_{\ln IM_i^g|rup_r}$ are the mean and variance of the natural logarithm of a known IM, IM_i, for a single rupture rup_r, and GMM gmm_g. The approximate case may be generalised to consider for many different rupture scenarios and GMMs, as a result the unconditional mean and variance are obtained using Eq. (3) and Eq. (4).

$$\mu_{\ln IM_i} = \sum_{r=1}^{n_{rup}} \sum_{g=1}^{n^r_{gmm}} p_r w_{r,g} \mu_{\ln IM_i^g|rup_r} \tag{3}$$

$$\sigma^2_{\ln IM_i} = \sum_{r=1}^{n_{rup}} \sum_{g=1}^{n^r_{gmm}} p_r w_{r,g} \left(\sigma^2_{\ln IM_i^g|rup_r} + \left(\mu_{\ln IM_i} - \mu_{\ln IM_i^g|rup_r} \right)^2 \right) \tag{4}$$

Lin et al. [3] classified these as exact and approximate approaches and introduced four methods for computing a target response spectrum, each differing based on the hazard input cases considered:

- Method 1 applies a single GMM to a single rupture scenario (i.e., $n_{rup} = n^r_{gmm} = 1$).
- Method 2 considers multiple GMMs for the same rupture scenario (i.e., $n_{rup} = 1, n^r_{gmm} > 1$). In this approach, GMM weights ($w_{1,g}$) are derived from the PSHA logic tree (i.e., $p_r = 1, w_{1,g} = w^l_{1,g}$, where l refers to the logic tree).
- Method 3 assigns a single rupture scenario to each GMM (i.e., $n_{rup} = n_{gmm} > 1$), with GMM weights ($w_{r,g}$) obtained from PSHA disaggregation (i.e., $p_r w_{r,g} = p^d_r w^d_{r,g}$, with d signifying disaggregation).
- Method 4 follows a generalised framework, adhering to the formulations in Eqs. (3) and (4).

These methods highlight varying levels of complexity and hazard input considerations in target response spectrum computation. Importantly, PSHA disaggregation weights (i.e., $p_r^d, w_{r,g}^d$) differ from logic tree weights (i.e., $p_r^l w_{r,g}^l$). Lin et al. [3] explain that logic tree weights function as prior weights in decision analysis, while disaggregation weights act as posterior weights. Additionally, disaggregation weights are typically expressed as a single product ($p_r^d w_{r,g}^d$), rather than separate components, yet remain consistent with the formulations in Eqs. (3) and (4), aligning with the *exact* approach. Figure 2 provides an example of the means and standard deviations of the unconditional target spectrum, calculated using Eq. (3) and Eq. (4). This example applies two rupture scenarios and two GMMs. The individual grey dashed branches represent results obtained from Eq. (1) for the means and Eq. (2) for the standard deviations.

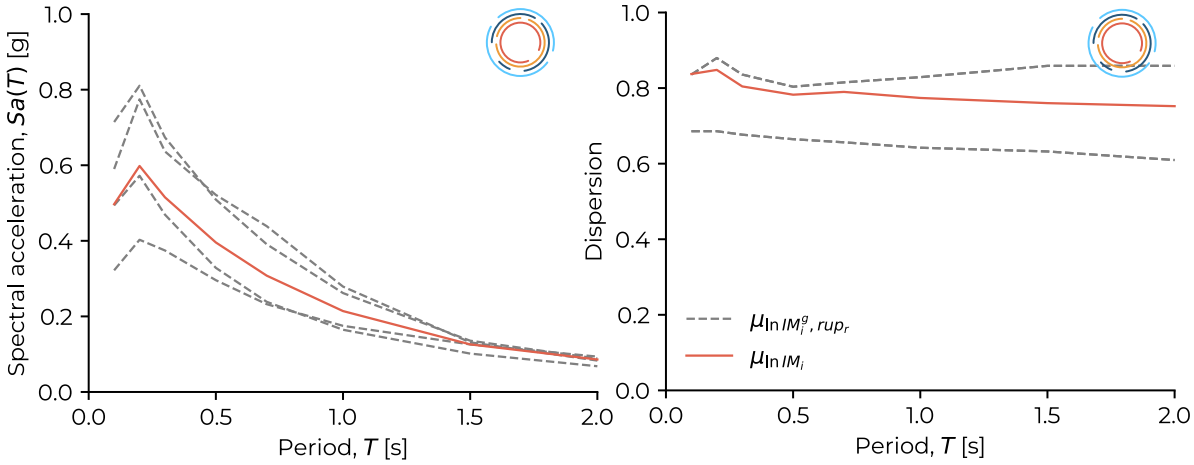

Figure 2. Illustration of (left) means and (right) dispersions computed for a case with two ruptures and two GMMs, where the solid lines represent the mean values, and the dashed lines represent the mean plus and minus two standard deviations for an unconditional selection.

3.2 Conditional spectrum

In the case of a conditional response spectrum dependent on a specific IM, denoted as *IM**, used as the target for record selection, the unconditional means and variances transform to $\mu_{\ln IM_i^g|\ln IM^{*h},rup_r}$ and $\sigma^2_{\ln IM_i^g|\ln IM^{*h},rup_r}$, respectively. It is assumed that the value of $\ln IM^{*h}$ will be obtained from another GMM, denoted as *h*. The conditional target mean and variance for a given rupture scenario, rup_r, and GMM pair are given by the following expression:

$$\mu_{\ln IM_i^g|\ln IM^{*h},rup_r} = \mu_{\ln IM_i^g|rup_r} + \rho_{\ln IM_i^g,\ln IM^{*h}|rup_r}\sigma_{\ln IM_i^g|rup_r}\epsilon_{\ln IM^{*h}|rup_r} \quad (5)$$

$$\sigma^2_{\ln IM_i^g|\ln IM^{*h},rup_r} = \sigma^2_{\ln IM_i^g|rup_r}\left(1-\rho^2_{\ln IM_i^g,\ln IM^{*h}|rup_r}\right) \quad (6)$$

$$\epsilon_{\ln IM^{*h}|rup_r} = \frac{\ln IM^* - \mu_{\ln IM^{*h}|rup_r}}{\sigma_{\ln IM^{*h}|rup_r}} \quad (7)$$

Baker [2] defines the term ρ as the correlation of the residuals, ϵ, between $\ln IM_i^g$ and $\ln IM^{*h}$, generalised here to correspond to two different GMMs, *g* and *h*, respectively, for a given rupture scenario rup_r. However, this requires that the correlation model, the GMMs, and the rupture parameters associated with these two IMs are available. In conditional selection described by Baker [2], these IMs are both spectral acceleration hence no distinction between GMMs is

needed; however, since the objective here to construct a generalised framework applicable to several IM types (i.e., GCIM), the generality is maintained. Baker and Bradley [31] proposed a more practical approach by suggesting the omission of dependence on specific rupture parameters and GMMs when developing correlation models. This simplification broadens the applicability of the correlation models without sacrificing their utility in practical situations. Consequently, Eq. (5) and Eq. (6) can be rewritten as Eq. (8) and Eq. (9), respectively.

$$\mu_{\ln IM_i^g|\ln IM^{*h},rup_r} = \mu_{\ln IM_i^g|rup_r} + \rho_{\ln IM_i,\ln IM^*}\sigma_{\ln IM_i^g|rup_r}\epsilon_{\ln IM^{*h}|rup_r} \tag{8}$$

$$\sigma^2_{\ln IM_i^g|\ln IM^*,rup_r} = \sigma^2_{\ln IM_i^g|rup_r}\left(1-\rho^2_{\ln IM_i,\ln IM^*}\right) \tag{9}$$

The combined conditional mean spectrum (CMS) is computed as the weighted sum of each:

$$\mu_{\ln IM_i^g|\ln IM^*,rup_r} = \sum_{h=1}^{n^r_{gmm}} w_h \mu_{\ln IM_i^g|\ln IM^{*h},rup_r} \tag{10}$$

In this case, the GMM h is considered independently, meaning that the weights w_h, must be derived from the logic tree branch for rup_r. For a single rupture scenario, the conditional mean and variance are given by Eq. (11) and Eq. (12), respectively.

$$\mu_{\ln IM_i|\ln IM^*} = \mu_{\ln IM_i^g|\ln IM^*,rup_r} \tag{11}$$

$$\sigma^2_{\ln IM_i|\ln IM^*} = \sigma^2_{\ln IM_i^g|\ln IM^*,rup_r} \tag{12}$$

Extending the conditional approach to include multiple rupture scenarios and GMMs, the resulting mean and variance are given by Eq. (13) and Eq. (14), respectively. This represents the full expansion of the GCIM approach for ground motion record selection, as proposed by Bradley [6]. The key distinction is the inclusion of multiple rupture scenarios, in contrast to the single rupture scenario originally presented in Bradley [6]. Figure 3 provides an example of the means and standard deviations of the conditional target spectrum, calculated using Eq. (13) and Eq. (14). This example applies two rupture scenarios and two GMMs. The individual grey dashed branches represent results obtained from Eq. (10) for the means and Eq. (9) for the standard deviations.

$$\mu_{\ln IM_i|\ln IM^*} = \sum_{r=1}^{n_{rup}}\sum_{g=1}^{n^r_{gmm}} p_r w_{r,g}\mu_{\ln IM_i^g|\ln IM^*,rup_r} \tag{13}$$

$$\sigma^2_{\ln IM_i|\ln IM^*} = \sum_{r=1}^{n_{rup}}\sum_{g=1}^{n^r_{gmm}} p_r w_{r,g}\left(\sigma^2_{\ln IM_i^g|\ln IM^*,rup_r} + \left(\mu_{\ln IM_i|\ln IM^*} - \mu_{\ln IM_i^g|\ln IM^*,rup_r}\right)^2\right) \tag{14}$$

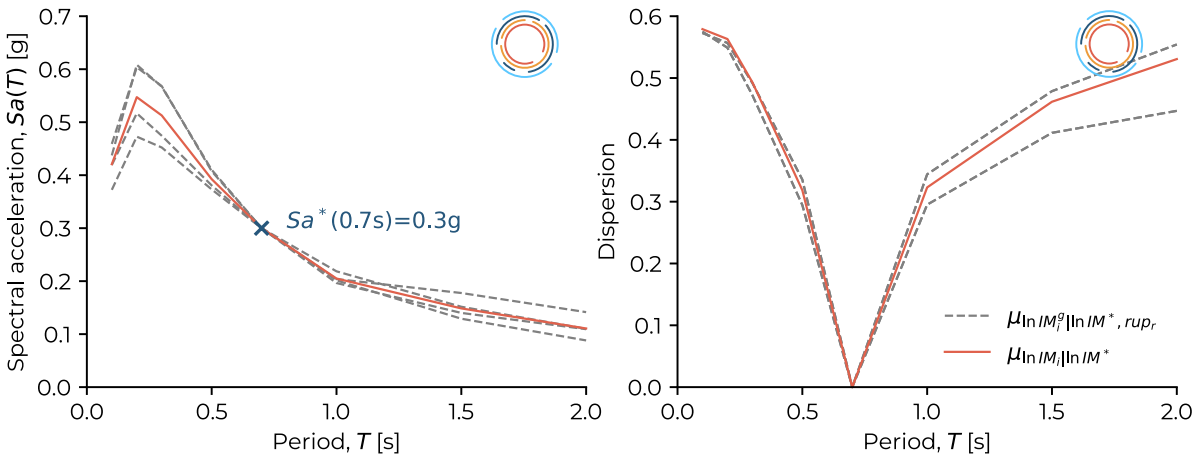

Figure 3. Illustration of (left) means and (right) dispersions computed for a case with two ruptures and two GMMs, where the solid lines represent the mean values, and the dashed lines represent the mean plus and minus two standard deviations for a conditional selection.

3.3 Simulating targets for ground motion record selection

Once the target means and variances are determined, whether they be for conditional or unconditional selection, ground motion records can be selected. The selection process is done collectively, meaning both the mean and variance of the group must be matched as a whole, rather than in a piecewise manner. To address this, Jayaram and Baker [32] proposed simulating suitable ground motion records $\ln IM_i$ and then searching for actual ground motions with values close to these simulated records. To achieve this, the vector of means, $\mu_{\ln\mathbf{IM}}$, and the covariance matrix, $\Sigma_{\ln\mathbf{IM}}$, for the vector of $\ln \mathbf{IM} = \{\ldots, \ln IM_i, \ldots\}$ are used. These can be written (for the case of conditional selection) as:

$$\mu_{\ln\mathbf{IM}} = \begin{bmatrix} \vdots \\ \mu_{\ln IM_i|\ln IM^*} \\ \vdots \end{bmatrix} \tag{15}$$

The standard deviation is written as:

$$\sigma_{\ln\mathbf{IM}} = \begin{bmatrix} \vdots \\ \sigma_{\ln IM_i|\ln IM^*} \\ \vdots \end{bmatrix} \tag{16}$$

The correlation between each of the $\ln\mathbf{IM}$ values, conditioned on $\ln IM^*$, must be computed to fully characterise the parameters of the multivariate normal distribution:

$$\rho = \begin{bmatrix} \ddots & \cdots & \\ \vdots & \rho_{\ln IM_i,\ln IM_j|\ln IM^*} & \vdots \\ & \cdots & \ddots \end{bmatrix} \tag{17}$$

where the individual conditional correlation term is given by:

$$\rho_{\ln IM_i,\ln IM_j|\ln IM^*} = \frac{\rho_{\ln IM_i,\ln IM_j} - \rho_{\ln IM_i,\ln IM^*}\rho_{\ln IM_j|\ln IM^*}}{\sqrt{1-\rho^2_{\ln IM_i|\ln IM^*}}\sqrt{1-\rho^2_{\ln IM_j|\ln IM^*}}} \tag{18}$$

This is then used to construct the covariance matrix between each of the $\ln\mathbf{IM}$ terms conditioned on $\ln IM^*$ as:

$$\Sigma = \begin{bmatrix} \ddots & \cdots & \\ \vdots & \Sigma_{\ln IM_i,\ln IM_j|\ln IM^*} & \vdots \\ & \cdots & \ddots \end{bmatrix} \tag{19}$$

where the individual conditional covariance term is given by:

$$\Sigma_{\ln IM_i,\ln IM_j|\ln IM^*} = \rho_{\ln IM_i,\ln IM_j|\ln IM^*}\sigma_{\ln IM_i|\ln IM^*}\sigma_{\ln IM_j|\ln IM^*} \tag{20}$$

3.4 Hazard consistency

One key parameter for assessing the suitability of a ground motion record set is its hazard consistency, as described by Lin et al. [33] for the case of spectral acceleration. The most straightforward validation involves ensuring that the selected ground motions align with the target IM^*. It is verified by checking that the IM* values for the selected records match the target values derived from PSHA. If the verification is successful, the records are considered hazard-consistent for this specific IM*. However, true hazard consistency extends beyond just

the single IM, it requires agreement across additional IMs. In the case of the conditional spectrum, this means evaluating spectral values beyond the conditioned period, but it should also incorporate different period-independent IMs. By ensuring consistency across multiple IMs, the selected records better capture the hazard characteristics of the site. This notion of hazard consistency is formally defined as:

$$\widetilde{H}(IM_i > y) = \int_x P(IM_i > y | IM^* = x) \, |dH(IM^*)|$$

where $H(IM^*)$ is the hazard curve of the conditioning IM* determined from PSHA and used to identify the ground motions, and $\widetilde{H}(IM_i > y)$ is the estimated hazard curve for some other IM_i based on the ground motion set that has been selected. This can be compared to the actual hazard curve determined from PSHA, $H(IM_i > y)$. If these are the same, the ground motion records can be said to be hazard-consistent for that IM_i, and analysts can benefit from a host of advantages regarding risk estimates, as described by Bradley [34] and Lin et al. [33].This includes the situation whereby when selecting ground motion records for multiple stripe analysis, and recurring issue regards which period of vibration to condition the selection on, with the first mode period of vibration being a popular choice when $IM^*=Sa(T)=Sa(T_1)$. When hazard consistency is ensured, this choice become much less relevant and analysts can proceed with more confidence in their results.

Figure 4 presents a sample record spectra of selected ground motion records and the associated hazard consistency plot obtained through the use of a tool available at https://apps.djura.it/hazard/hazard-consistency. The ground motion records are conditioned on a $IM^*=Sa(T=0.7s)$, but are checked for hazard consistency at other periods $IM_i = Sa(T_i)$, where T_i is 0.5s, 1s, 1.5, and 2s. It should be noted that hazard consistency is not always an easy criterion to satisfy, and depends on several factors, such as the use of *approximate* versus *exact* conditioning of the target spectra (see Section 3.2), the suitability of the assumption that correlation models are actually rupture and ground motion model independent, in addition to the natural error between the selected ground motion records and the target (Section 6 below). Relaxing any of these criteria in ground motion selection undoubtedly makes identifying suitable records much easier and efficient, but these slight discrepancies with respect to the "true" hazard are accumulated and collectively visible in a check such as that shown below.

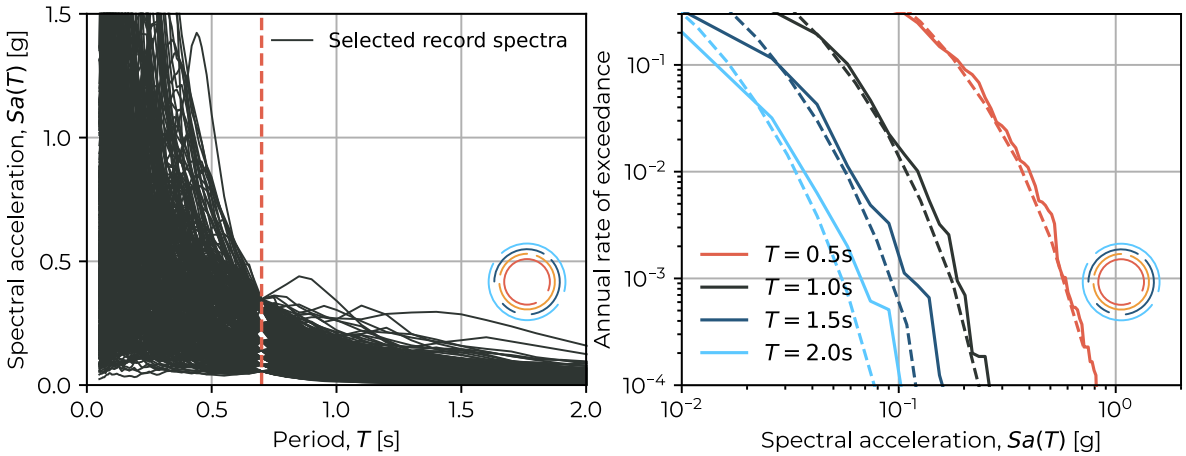

Figure 4. (left) sample record spectra of selected records and (right) the associated hazard consistency plot

4 GROUND MOTION RECORD SELECTION TOOL

This section presents an online toolbox developed to implement the outlined framework. The tool, available at https://apps.djura.it/hazard/record-selector, currently supports several methods, ranging from basic building code requirements to more complex hazard scenarios. However, this section will not focus on the building code requirements, which is mentioned in Section 6 below. The tool allows for the selection of records using a set of target spectra for various ground motion IMs, based on specific rupture parameters commonly referred to as scenario-based analysis. Both generalized unconditional (Section 3.1) and conditional (Section 3.2) selection options are provided. Within the tool, users are prompted to select key attributes and functionalities such as:

1. **IM – GMM Pairs**: IMs must be specified alongside the GMMs required to predict their expected distribution. Figure 5(left) illustrates the interface for this process. For example, when spectral acceleration, $Sa(T)$, is selected, a menu of available GMMs is displayed. The graphic below updates dynamically to reflect the chosen GMMs and shows their associated weights, which users can adjust as needed. The tool currently supports the following IMs: $Sa(T)$, average spectral acceleration, $Sa_{avg}(T)$, PGA, peak ground velocity, PGV, significant durations, Ds_{575} and Ds_{595}), and filtered incremental velocity, $FIV3$.
2. **Rupture Scenarios**: Rupture parameters are defined based on the chosen IMs and GMMs. Site-specific characteristics, separate from the earthquake rupture itself, are also defined. The most common parameter for site characterization is the average shear wave velocity to 30 meters depth, Vs_{30}. Depending on the selected GMMs, additional fields such as $Z_{2.5}$ and the soil/rock classification will also appear. The interface provides detailed explanations for each parameter, along with references. Next, rupture parameters are typically derived from PSHA disaggregation results. Users often specify a single dominant rupture scenario for each intensity level, following the approximate selection method (Lin et al. [3]). A key feature of this tool is its ability to handle multiple rupture scenarios, assigning weights to each based on PSHA results, which aligns with the exact approach outlined by Lin et al. [3]. Figure 5(right) shows the graphical interface for this process.
3. **Conditional IM (for conditional selection only)**: The fundamental concept behind conditional ground motion record selection is ensuring that the selected motions match a specified intensity value for a given IM. This intensity value, called the conditioning value or IM*, is typically derived from the hazard curve or PSHA. After selecting the IMs in Step 1, the user must specify which IM to condition on and its corresponding value. The tool then utilises this value to define the target distribution of the selected ground motions relative to the conditioning point.
4. **Logic Tree**: Once the scenarios are configured and the inputs finalised, the logic tree can be visualised. This directs the user to a dedicated page where all relevant details such as the IMs, GMMs, weights, and rupture scenarios are displayed in a comprehensive table (Figure 6). This ensures that all aspects of the analysis are clearly organised and easy to access. For a more intuitive overview, an interactive logic tree diagram (Figure 7) provides a global visual representation of the analysis. The diagram breaks down the various components, starting with the rupture scenarios (two are shown in the example). For each rupture scenario, it displays the predicted IMs and the associated GMMs used to estimate their distributions. By hovering over specific elements, users can view the weights assigned to each IM and GMM. The logic tree is flexible, allowing users to expand or collapse sections to adjust the level of

detail. Moreover, both the full logic tree and the interactive diagram can be downloaded for offline access, providing a convenient way to store and review the inputs and results.

5. **Advanced Input**: The software offers several advanced configuration options, with default values set for convenience. These include selecting the number of horizontal components and the method used to define them (geomean, RotD100, RotD50). Users can modify the number of ground motions, set scaling limits, and define computational settings, such as the number of iterations required to achieve a close match between the target distribution and the selected ground motions. Additionally, users can add more IM definitions, for example, specifying $Sa(T)$ at a particular period T, with the option to assign importance weights to each IM. Further, the limits for earthquake rupture parameters can be customised to refine the ground motion selections, such as restricting the range of magnitudes or faulting styles.

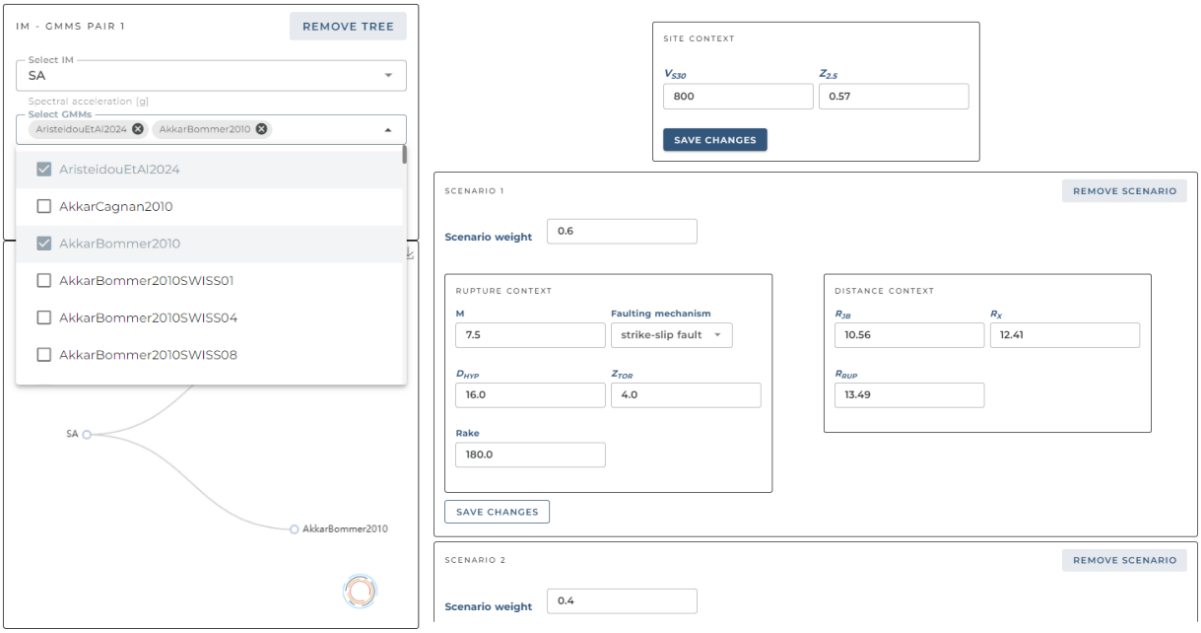

Figure 5. Graphical UI of the proposed tool: (left) IM-GMM pair selection, (right) Rupture scenario definition.

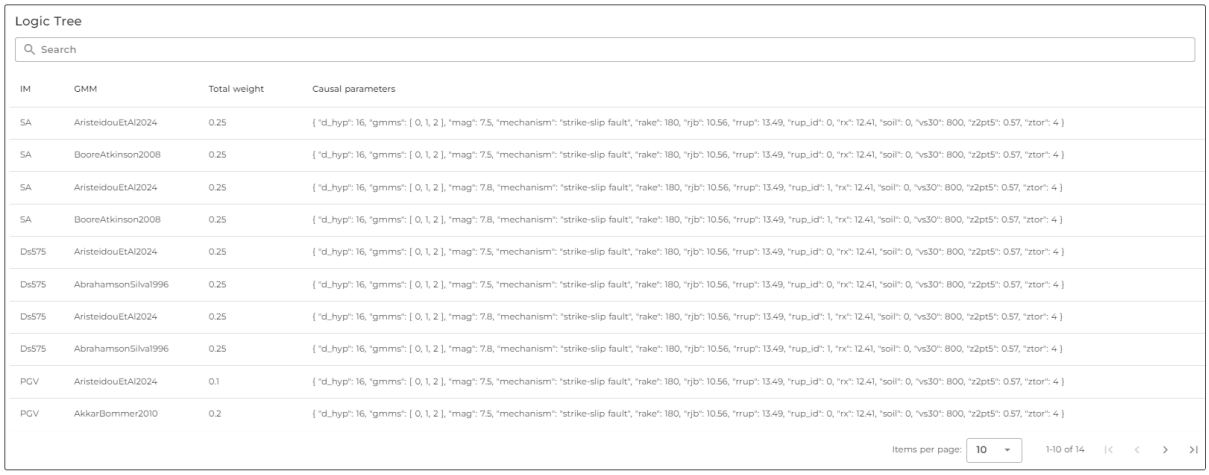

Figure 6. Logic tree table listing relevant data in a structured format.

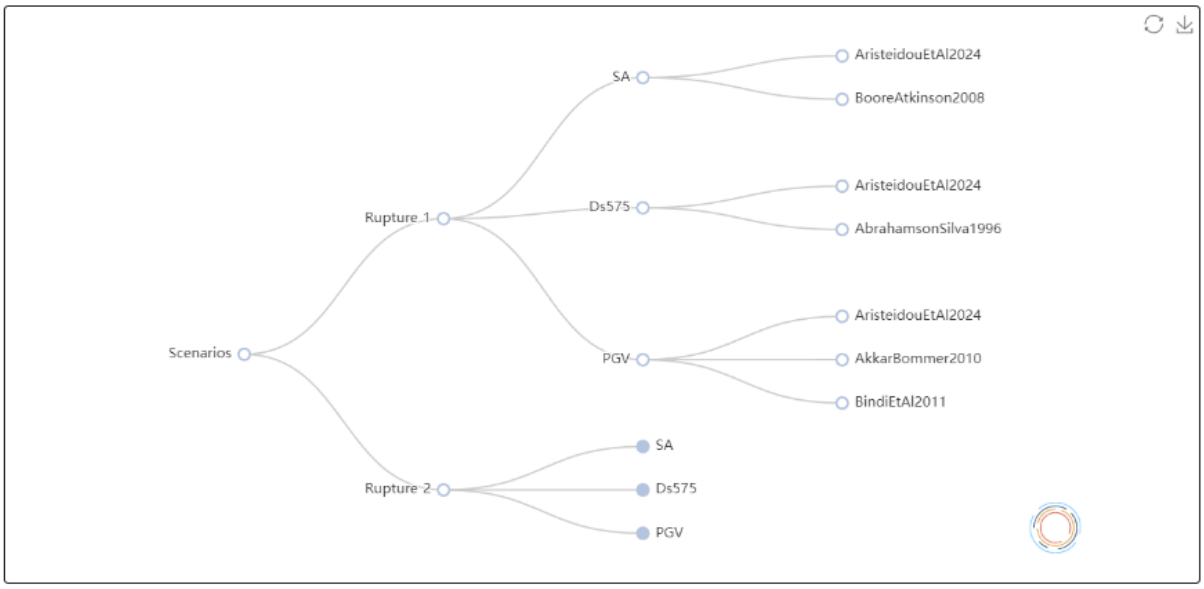

Figure 7. Interactive logic tree diagram.

It is crucial to highlight that at each stage of input configuration and output generation, data can be downloaded for use in other applications or analyses, and can also be queried via API calls that allows for more automated and widespread usage.

5 EXAMPLE RECORD SELECTION

5.1 Special case: SA(T)-based unconditional and conditional selection

This section presents an example application of the tool, utilising the framework outlined in Sections 3 and 4. The tool is applied to perform selection using both methods: unconditional and conditional using only SA as the IM. Once all input data is defined, the tool generates a target distribution. Figure 8(left) shows an example of a target unconditional distribution, while Figure 8(right) illustrates a target conditional distribution, where IM* corresponds to *Sa*(0.7s) with a value of 0.3g. For the sample calculation, the scaling factors for the records were limited to 3.0, and event magnitudes were constrained to a minimum of 5.

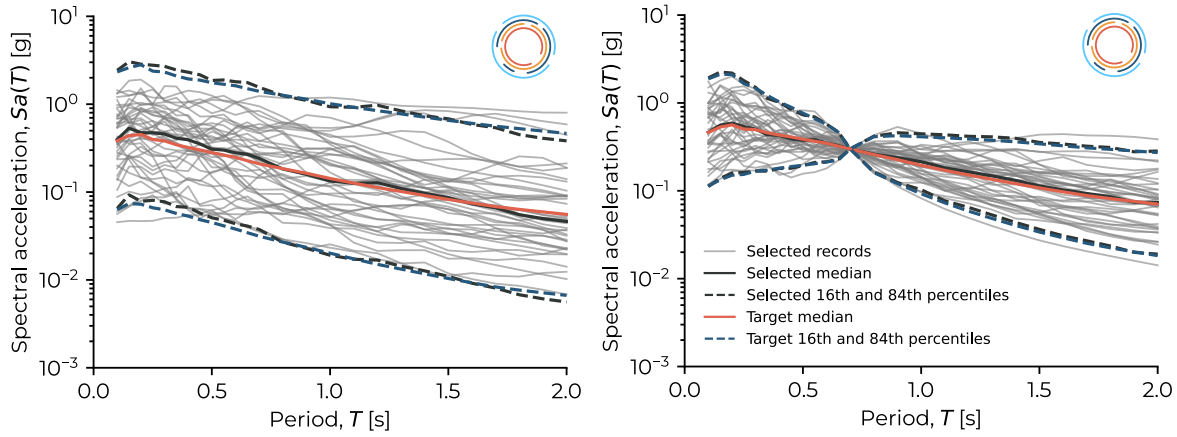

Figure 8. (left) unconditional and (right) conditional target distributions.

In addition to the target distributions, Figure 8 also displays the selected record spectra alongside their median spectra. Each selected ground motion record spectrum is presented with its mean and standard deviations, which, as shown, align with the median and standard deviation of the target distributions. For each relevant IM, Kolmogorov-Smirnov (KS) goodness-of-fit tests are performed to evaluate the quality of the selection. The KS test compares the absolute difference between the theoretical cumulative distribution function (CDF) and the empirical distribution function (EDF) of the sample [35]. Figure 9 shows the results of some of the *SA*(*T*) tests, demonstrating that the EDFs of the selected ground motions closely match the target distribution and its KS bounds at a 5% significance level. Finally, the ground motion record suite can be downloaded in a single ZIP file for further analysis along with the metadata of the records.

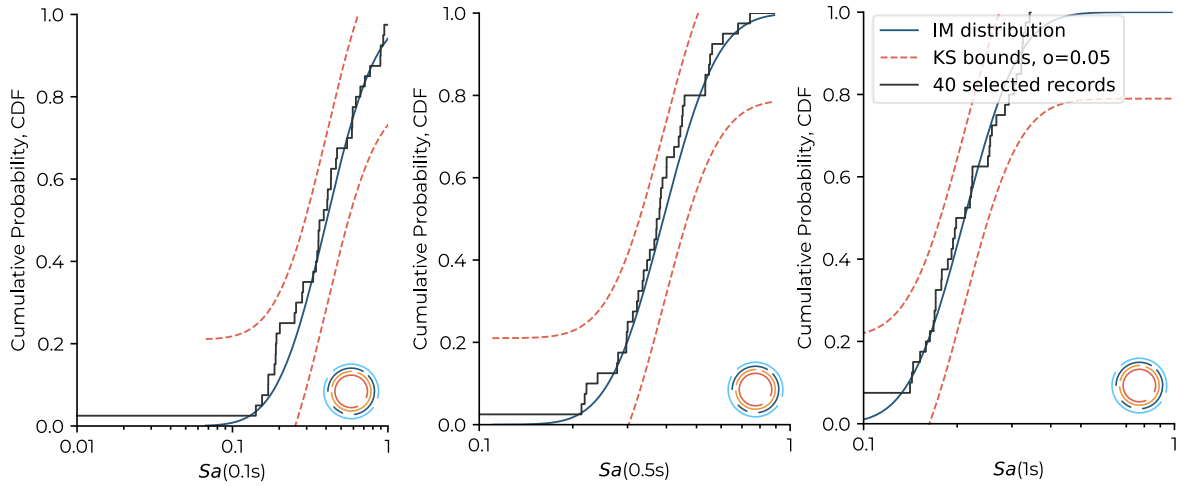

Figure 9. Illustration of the KS tests for a select set of *SA*(*T*)-based IMs following the conditional selection.

For this particular scenario, only *SA*(*T*)-based IMs were considered during selection, while any other IM type was ignored. To visualise the impact of ignoring certain IMs during selection, *SA*(0.1s) was ignored as well along with *FIV*3(*T*)-based IMs and Ds_{575}. As a result, those IMs fail the KS tests. While *FIV*3(2s) passes, the EDF of the selected records approaches the KS bounds, suggesting that under a different selection scenario, the condition might not have been met. Figure 10 demonstrates how the EDFs of the selected ground motions are not within the KS bounds at a 5% significance level. To remedy it, and achieve hazard consistency for all IMs of interest a general case of considering all types of IMs is considered in the following section.

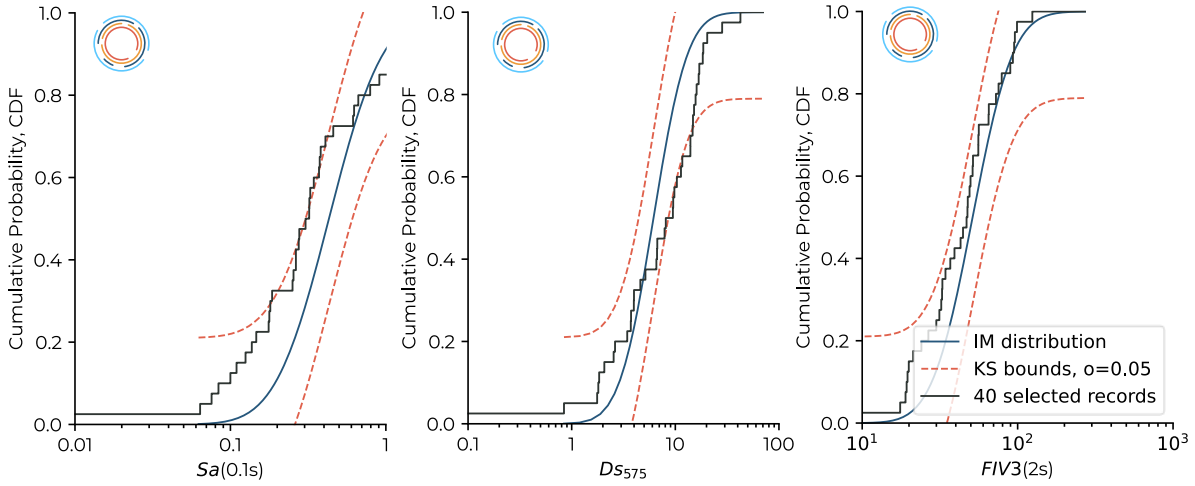

Figure 10. Illustration of the KS tests for a select set of IMs ignored during conditional selection.

5.2 General case: Record selection using multiple types of IMs

Similarly, an example application of the tool is presented, but for a general case scenario using multiple types of IMs, such as *SA*(*T*), *FIV*3(*T*) and Ds_{575}. The tool is applied to perform selection using both methods: unconditional and conditional. Figure 11(left) shows an example of a target unconditional distribution, while Figure 11(right) illustrates a target conditional distribution, where IM* corresponds to *Sa*(0.7s) with a value of 0.3g. For the sample calculation, the scaling factors for the records were limited to 3.0, and event magnitudes were constrained to a minimum of 5.

Figure 12 shows the results of some of the IM tests, demonstrating that the EDFs of the selected ground motions closely match the target distribution and its KS bounds at a 5% significance level. This is also the case for other significant duration and *FIV*3 type IMs, essentially meaning that a GCIM approach has been carried out. If all IM types were not considered during selection, these distributions may not match the target distribution, implying a lack of hazard consistency as seen previously in Figure 10. These issues can introduce notable bias in structural response analysis results as reported in several past studies [e.g., [12], [36], [37]]. Finally, the ground motion record suite can be downloaded in a single ZIP file for further analysis along with the metadata of the records.

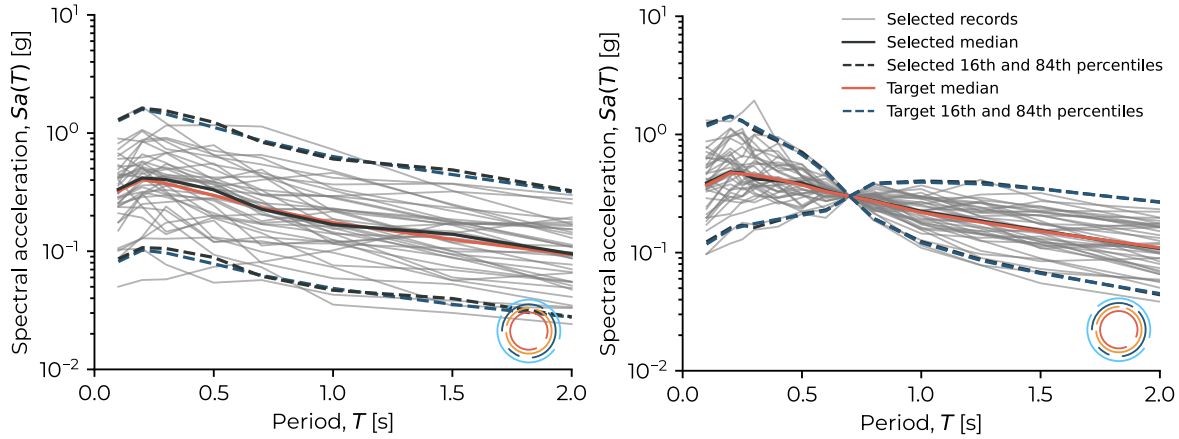

Figure 11. (left) unconditional and (right) conditional target distributions.

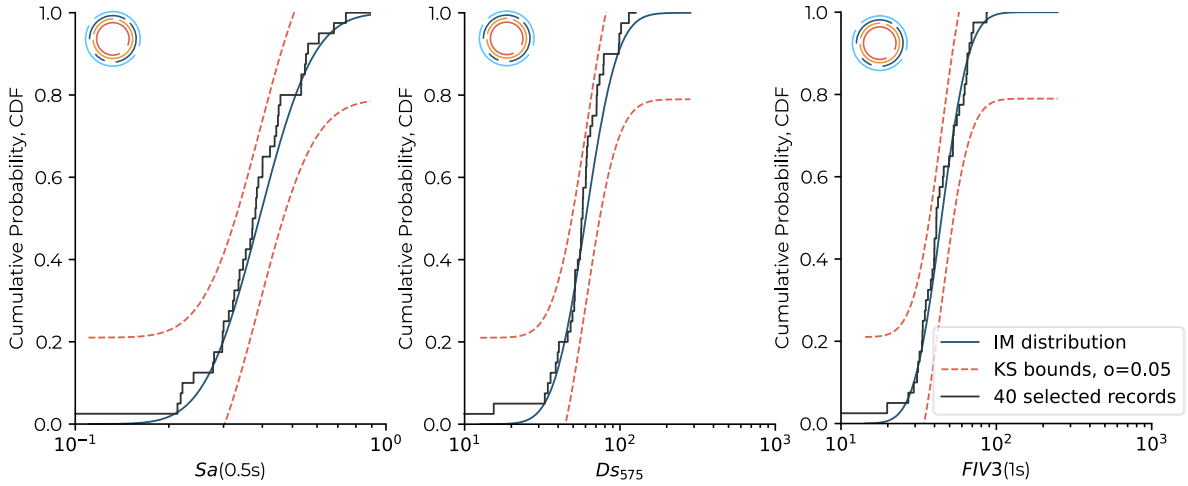

Figure 12. Illustration of the KS tests for a select set of IMs following the conditional selection.

While it may seem evident, it is worth emphasising that no other widely available software tool currently performs such a comprehensive ground motion record selection. In other words, the tool enables the targeting of ground motion characteristics such as spectral acceleration, velocity, and duration to align with the seismic hazard specific to a given site. This means the selected records are highly representative of the site's seismic hazard, based on PSHA results. The advantage of this approach is that the chosen records are expected to yield more efficient outcomes (i.e., reduced dispersion in structural response), while also eliminating potential biases in results due to ground motion characteristics often overlooked by practitioners, primarily because suitable tools have not been available until now.

6 GROUND MOTION RECORD SELECTION IN BUILDING CODES

To streamline code-based record selection, an online toolbox has been developed and is accessible at https://apps.djura.it/hazard/record-selector/uhs. To maintain conciseness, this section provides a focused discussion on key aspects of the methodology. While the toolbox supports a wide range of functionalities and code-based spectra (e.g., [29], [38]–[40]), only the target elastic acceleration response spectrum from Eurocode 8 [41] is highlighted here. Additional details on other implemented spectra and planned enhancements are available within the toolbox interface. Typically, the target response spectrum is based on the reference peak ground acceleration (PGA) on rock, which is to be determined from a suitable seismic hazard study or reference document, and is intended to be representative of a UHS. In addition, the importance class of the building, for which record selection is performed, the ground type and type of response spectrum are required. The derived response spectrum corresponds to the one used for the no-collapse requirement. Finally, once the constraints on scaling factors are set and the period bounds for error minimisation are defined based on structure's dynamic properties, the three-component record selection and scaling process are conducted. Figure 13 illustrates a sample selection based on the identified target spectrum for both horizontal and vertical components.

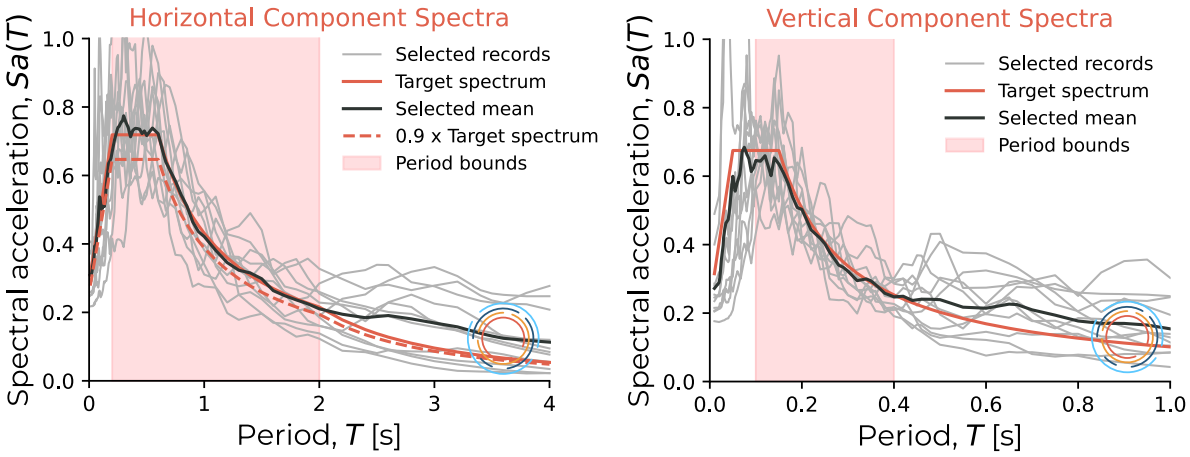

Figure 13. EC8-based record selection for (left) horizontal and (right) vertical component spectra.

7 SUMMARY

This paper presents an intuitive software tool designed to simplify the process of selecting ground motion records for seismic design and assessment. By harnessing recent advancements in computational capabilities, the tool incorporates building code-based record selection as well as state-of-the-art methods such as the generalised conditional intensity measure (GCIM) framework, enabling efficient record selection from harmonised databases like PEER NGA-West2. It supports the use of multiple ground motion models (GMMs) and Intensity Measures (IMs), integrating cross-correlation matrices similar to those used in probabilistic seismic hazard analysis (PSHA). The tool provides flexibility in selecting both horizontal and vertical ground motion components and features an interface that facilitates easy switching between selection methods, while also allowing users to store and retrieve input and output data seamlessly. A case study illustrated the tool's ability to perform both conditional and unconditional ground motion selection. The approach aligns with industry standards, producing a ground motion suite that matched the target distribution and passed all Kolmogorov-Smirnov goodness-of-fit tests for all relevant IMs. This ensures the selected ground motions accurately reflect real-world conditions, making the tool particularly valuable for site-specific studies and advanced ground motion selection methods as specified in design codes.

REFERENCES

[1] C. A. CORNELL, “Engineering Seismic Risk Analysis, Bull. Seismol. Soc. Am. 58, 1583–1606.,” *Bull. Seismol. Soc. Am.*, vol. 58, no. 5, pp. 1583–1606, 1968, [Online]. Available: http://bssa.geoscienceworld.org/cgi/content/abstract/58/5/1583%5Cnhttp://bssaonline.org/cgi/content/abstract/58/5/1583

[2] J. W. Baker, “Conditional mean spectrum: Tool for ground-motion selection,” *J. Struct. Eng.*, vol. 137, no. 3, pp. 322–331, 2011, doi: 10.1061/(ASCE)ST.1943-541X.0000215.

[3] T. Lin, S. C. Harmsen, J. W. Baker, and N. Luco, “Conditional Spectrum Computation Incorporating Multiple Causal Earthquakes and Ground-Motion Prediction Models,” *Bull. Seismol. Soc. Am.*, vol. 103, no. 2A, pp. 1103–1116, Apr. 2013, doi: 10.1785/0120110293.

[4] N. Jayaram, T. Lin, and J. W. Baker, "A Computationally Efficient Ground-Motion Selection Algorithm for Matching a Target Response Spectrum Mean and Variance," *Earthq. Spectra*, vol. 27, no. 3, pp. 797–815, Aug. 2011, doi: 10.1193/1.3608002.

[5] G. Wang, "A ground motion selection and modification method capturing response spectrum characteristics and variability of scenario earthquakes," *Soil Dyn. Earthq. Eng.*, vol. 31, no. 4, pp. 611–625, Apr. 2011, doi: 10.1016/j.soildyn.2010.11.007.

[6] B. A. Bradley, "A generalized conditional intensity measure approach and holistic ground-motion selection," *Earthq. Eng. Struct. Dyn.*, vol. 39, no. 12, pp. 1321–1342, Oct. 2010, doi: 10.1002/eqe.995.

[7] B. A. Bradley, "A ground motion selection algorithm based on the generalized conditional intensity measure approach," *Soil Dyn. Earthq. Eng.*, vol. 40, pp. 48–61, Sep. 2012, doi: 10.1016/j.soildyn.2012.04.007.

[8] L. Eads, E. Miranda, H. Krawinkler, and D. G. Lignos, "An efficient method for estimating the collapse risk of structures in seismic regions," *Earthq. Eng. Struct. Dyn.*, vol. 42, no. 1, pp. 25–41, Jan. 2013, doi: 10.1002/eqe.2191.

[9] A. M. B. Nafeh and G. J. O'Reilly, "Fragility functions for non-ductile infilled reinforced concrete buildings using next-generation intensity measures based on analytical models and empirical data from past earthquakes," *Bull. Earthq. Eng.*, vol. 22, no. 10, pp. 4983–5021, Aug. 2024, doi: 10.1007/s10518-024-01955-4.

[10] A. M. B. Nafeh and G. J. O'Reilly, "Unbiased simplified seismic fragility estimation of non-ductile infilled RC structures," *Soil Dyn. Earthq. Eng.*, vol. 157, no. March, p. 107253, 2022, doi: 10.1016/j.soildyn.2022.107253.

[11] M. Kohrangi, D. Vamvatsikos, and P. Bazzurro, "Site dependence and record selection schemes for building fragility and regional loss assessment," *Earthq. Eng. Struct. Dyn.*, vol. 46, no. 10, pp. 1625–1643, 2017, doi: 10.1002/eqe.2873.

[12] G. J. O'Reilly, "Limitations of Sa(T1) as an intensity measure when assessing non-ductile infilled RC frame structures," *Bull. Earthq. Eng.*, vol. 19, no. 6, pp. 2389–2417, Apr. 2021, doi: 10.1007/s10518-021-01071-7.

[13] G. J. O'Reilly, "Seismic intensity measures for risk assessment of bridges," *Bull. Earthq. Eng.*, vol. 19, no. 9, pp. 3671–3699, Jul. 2021, doi: 10.1007/s10518-021-01114-z.

[14] G. J. O'Reilly and D. Shahnazaryan, "On the utility of story loss functions for regional seismic vulnerability modeling and risk assessment," *Earthq. Spectra*, vol. 40, no. 3, pp. 1933–1955, Aug. 2024, doi: 10.1177/87552930241245940.

[15] A. M. B. Nafeh and G. J. O'Reilly, "Simplified pushover-based seismic loss assessment for existing infilled frame structures," *Bull. Earthq. Eng.*, vol. 22, no. 3, pp. 951–995, Feb. 2024, doi: 10.1007/s10518-023-01792-x.

[16] H. Dávalos and E. Miranda, "Filtered incremental velocity: A novel approach in intensity measures for seismic collapse estimation," *Earthq. Eng. Struct. Dyn.*, vol. 48, no. 12, pp. 1384–1405, Oct. 2019, doi: 10.1002/eqe.3205.

[17] H. Dávalos and E. Miranda, "Evaluation of FIV3 as an Intensity Measure for Collapse Estimation of Moment-Resisting Frame Buildings," *J. Struct. Eng.*, vol. 146, no. 10, Oct. 2020, doi: 10.1061/(ASCE)ST.1943-541X.0002781.

[18] S. Aristeidou and G. J. O'Reilly, "Exploring the Use of Orientation-Independent

Inelastic Spectral Displacements in the Seismic Assessment of Bridges," *J. Earthq. Eng.*, vol. 28, no. 12, pp. 3515–3538, Sep. 2024, doi: 10.1080/13632469.2024.2343067.

[19] B. A. Bradley, "Empirical equations for the prediction of displacement spectrum intensity and its correlation with other intensity measures," *Soil Dyn. Earthq. Eng.*, vol. 31, no. 8, pp. 1182–1191, Aug. 2011, doi: 10.1016/j.soildyn.2011.04.007.

[20] K. Afshari and J. P. Stewart, "Physically Parameterized Prediction Equations for Significant Duration in Active Crustal Regions," *Earthq. Spectra*, vol. 32, no. 4, pp. 2057–2081, Nov. 2016, doi: 10.1193/063015EQS106M.

[21] K. W. Campbell and Y. Bozorgnia, "Ground Motion Models for the Horizontal Components of Arias Intensity (AI) and Cumulative Absolute Velocity (CAV) Using the NGA-West2 Database," *Earthq. Spectra*, vol. 35, no. 3, pp. 1289–1310, Aug. 2019, doi: 10.1193/090818EQS212M.

[22] H. Zafarani and M. R. Soghrat, "Ground Motion Models for Non-Spectral Intensity Measures Based on the Iranian Database," *J. Earthq. Eng.*, vol. 27, no. 13, pp. 3786–3806, Oct. 2023, doi: 10.1080/13632469.2022.2150334.

[23] H. Dávalos, P. Heresi, and E. Miranda, "A ground motion prediction equation for filtered incremental velocity, FIV3," *Soil Dyn. Earthq. Eng.*, vol. 139, p. 106346, Dec. 2020, doi: 10.1016/j.soildyn.2020.106346.

[24] H. Dávalos and E. Miranda, "A Ground Motion Prediction Model for Average Spectral Acceleration," *J. Earthq. Eng.*, vol. 25, no. 2, pp. 319–342, Jan. 2021, doi: 10.1080/13632469.2018.1518278.

[25] L. Eads, E. Miranda, and D. G. Lignos, "Average spectral acceleration as an intensity measure for collapse risk assessment," *Earthq. Eng. Struct. Dyn.*, vol. 44, no. 12, pp. 2057–2073, Sep. 2015, doi: 10.1002/eqe.2575.

[26] S. Aristeidou, D. Shahnazaryan, and G. J. O'Reilly, "Artificial neural network-based ground motion model for next-generation seismic intensity measures," *Soil Dyn. Earthq. Eng.*, vol. 184, p. 108851, Sep. 2024, doi: 10.1016/j.soildyn.2024.108851.

[27] S. Aristeidou, D. Shahnazaryan, and G. J. O'Reilly, "Correlation models for next-generation amplitude and cumulative intensity measures using artificial neural networks," *Earthq. Spectra*, Oct. 2024, doi: 10.1177/87552930241270563.

[28] J. J. Bommer and R. Pinho, "Adapting earthquake actions in Eurocode 8 for performance-based seismic design," *Earthq. Eng. Struct. Dyn.*, vol. 35, no. 1, pp. 39–55, Jan. 2006, doi: 10.1002/eqe.530.

[29] CEN, *Design of Structures for Earthquake Resistance (Draft) - Part 1-1: General Rules, Seismic Actions and Rules (EN 1998-1-1:2024)*. 2024.

[30] T. D. Ancheta *et al.*, "NGA-West2 database," *Earthq. Spectra*, vol. 30, no. 3, pp. 989–1005, 2014, doi: 10.1193/070913EQS197M.

[31] J. W. Baker and B. A. Bradley, "Intensity Measure Correlations Observed in the NGA-West2 Database, and Dependence of Correlations on Rupture and Site Parameters," *Earthq. Spectra*, vol. 33, no. 1, pp. 145–156, Feb. 2017, doi: 10.1193/060716eqs095m.

[32] N. Jayaram and J. W. Baker, "Efficient sampling and data reduction techniques for probabilistic seismic lifeline risk assessment," *Earthq. Eng. Struct. Dyn.*, vol. 39, no. 10, pp. 1109–1131, Aug. 2010, doi: 10.1002/eqe.988.

[33] T. Lin, C. B. Haselton, and J. W. Baker, "Conditional spectrum-based ground motion selection . Part I : Hazard consistency for risk-based assessments," no. June, pp. 1847–1865, 2013, doi: 10.1002/eqe.

[34] B. A. Bradley, "The seismic demand hazard and importance of the conditioning intensity measure," *Earthq. Eng. Struct. Dyn.*, vol. 41, no. 11, pp. 1417–1437, Sep. 2012, doi: 10.1002/eqe.2221.

[35] A. H.-S. Ang and W. H. Tang, *Probability Concepts in Engineering: Emphasis on Applications in Civil and Environmental Engineering.* New York, NY: Wiley, 2006.

[36] R. Chandramohan, J. W. Baker, and G. G. Deierlein, "Quantifying the Influence of Ground Motion Duration on Structural Collapse Capacity Using Spectrally Equivalent Records," *Earthq. Spectra*, vol. 32, no. 2, pp. 927–950, May 2016, doi: 10.1193/122813eqs298mr2.

[37] S. Aristeidou, "Advances in the practical application of next-generation intensity measures for efficient seismic risk assessment," IUSS Pavia; Italy., 2025.

[38] CEN, *Eurocode 8: design of structures for earthquake resistance, Part 1, General Rules, Seismic Actions and Rules for Buildings*. Brussels, Belgium: European Committee for Standardization (CEN), 2004.

[39] ASCE 7-22, *Minimum Design Loads And Associated Criteria For Buildings*. 2022.

[40] NTC, "Norme Tecniche Per Le Costruzioni," Rome, Italy, 2018.

[41] CEN, "Eurocode 8: Design of Structures for Earthquake Resistance - Part 1: General Rules, Seismic Actions and Rules for Buildings (EN 1998-1:2004)," Brussels, Belgium, Comité Européen de Normalisation, 2004.